ELSEVIER

Syntheses and structures of non-symmetric guanidinato zirconium and hafnium complexes and their catalytic behavior for ethylene polymerization

Meisu Zhou, Hongbo Tong, Xuehong Wei, Diansheng Liu *

Institute of Applied Chemistry, Shanxi University, Taiyuan 030006, PR China

Abstract

Equivalent addition reactions of PhN(Li)SiMe$_3$ to nitriles, RCN (R = dimethylamido, 1-piperidino), generated non-symmetric guanidinato lithium [(Et$_2$O)LiN(SiMe$_3$)C(NMe$_2$)N(Ph)]$_2$ (**1**) or [(THF)LiN(SiMe$_3$)C(NMe$_2$)N(Ph)]$_2$ (**2**) and [(Et$_2$O)LiN(SiMe$_3$)C-(N(CH$_2$)$_5$)N(Ph)]$_2$ (**5**) which further reacted with zirconium or hafnium tetrachloride to form Zr and Hf guanidinato complexes with the general formula [PhNC(R)NSiMe$_3$]$_3$MCl (R = dimethylamido, M = Zr (**3**), Hf (**4**); R = 1-piperidino, M = Zr (**6**), Hf (**7**)). Complexes **1**–**4**, **6** and **7** were well characterized by ^{1}H, ^{13}C NMR and microanalysis, the single crystal X-ray diffraction analysis data for complexes **1**, **3**, **4** and **7** were also provided. Furthermore, complexes **3**, **4**, **6** and **7** were found to be active for ethylene polymerization. The influences of cocatalyst, pressure, reaction temperature and Al/M ratio on activity were investigated.
© 2007 Elsevier B.V. All rights reserved.

Keywords: Guanidinato complexes; Synthesis; Structure; Ethylene polymerization

1. Introduction

Both of guanidine and amidine compounds have received increased attentions from 1980s because of their steric and electronic flexibility, the variety of possible coordination modes. Especially for guanidines, they can form neutral, monoanionic [(RN)$_2$CNR$_2$]$^-$ or dianionic [(RN)$_3$C]$^{2-}$ forms. These features mean that guanidinates have the potential to develop into valuable ancillary ligands in coordination and organometallic chemistry [1]. Beyond the fundamental investigation of guanidinate complexes related to their structural features, some guanidinato complexes have been identified as initiators or catalysts for polymerization reactions, e.g., trimethylene carbonate and its copolymerization with ε-caprolactone [2], the polymerization of lactide [3], the polymerization of α-olefins [3], or the polymerization of styrene [4]. Regarding to the com-

plexes of group IVB, the wide investigations have recognized that they could be used as the alternatives of unique cyclopentadienyl species in order to form suitable catalytic sites for the polymerization of α-olefins [5–8], furthermore, zirconium complexes with co-ligands of amidinato and Cp ring showed some special intramolecular reactivity and extreme activities for the living polymerization of (sterically encumbered) α-olefins at low temperature [9]. Guanidinate-supported titanium imido complexes were prepared and firstly used as a catalyst for alkyne hydroamination [10]. Recently, zirconium-amido guanidinato complex was used as a potential precursor for the CVD of ZrO$_2$ thin films [11].

The first linked guanidinato ligand system and its Ti and Zr complexes were synthesized and demonstrated that the two of guanidinato moieties resulted in changes to ligand geometry and metal coordination behavior and difference of the reactivity from unlinked analogues [12]. Our previous works involved the β-diketiminato and amidinato metal complexes, which were prepared from the reaction

---

of amido anions with nitriles and had the electronic properties of the delocalized π-electrons [13–18]. Some early and late transition metal complexes were studied for the consideration of potential precursors in ethylene polymerization [13]. In this work, the addition reactions of PhN(Li)SiMe₃ to nitriles were carried out to generate non-symmetric guanidinato lithium, which reacted with zirconium and hafnium tetrachloride provides a series of triguanidinato Zr(IV) or Hf(IV) chloride, respectively. The zirconium and hafnium metal complexes showed moderate catalytic activity in ethylene polymerization.

2. Results and discussion

2.1. Synthesis and characterization of complexes 1–7

The symmetric guanidinate ligand and complexes were commonly studied because they could be easily formed by an insertion reaction of carbodiimides RN=C=NR into a metal alkyl amide bond [19–22]. Our non-symmetric guanidine ligands, [N(Ph)–C(R)–N(SiMe₃)]Li (1, R = NMe₂, 5, 1-piperidino), were prepared from the reaction of PhN(Li)SiMe₃ with dimethylcyanmide or 1-piperidinecarbonitrile. The synthetic routes to complexes 1–7 are illustrated in Scheme 1.

Treatment of PhN(Li)SiMe₃ with (CH₃)₂NCN in *n*-hexane and recrystallization from Et₂O gave complex 1 as colorless crystals in 80% yield. Complex 2 was obtained in 44% yield from the reaction of PhN(Li)SiMe₃ with (CH₃)₂NCN in THF and recrystallized from THF as well. The colorless crystalline complex 2 was very air-sensitive and changed into red when it exposed to air. The lithium salt 5 was not isolated but was generated *in situ* in similar procedure to complex 1.

The non-symmetric guanidine ligands were designed to form complex with zirconium and hafnium for the consideration of potential precursor for the polymerization of ethylene. However, attempts for the equivalent ligand/metal complexes with formula of LMCl₃ (M = Zr or Hf) from the reactions of 1 with an equivalent portion of MCl₄ in THF at −78 °C were not successful. So did the equivalent reaction of 5 with ZrCl₄ or HfCl₄, even no matter THF or Et₂O as solvent could not help the reaction for available complexes. Therefore the reactions with different molar ratio of guanidinato ligands to MCl₄ are explored and finally reproducible reaction with good yield of complexes with molar ratio of guanidinato lithium to MCl₄ as 3:1 was carried out in THF or hexane. The reaction of 1 with one third molar ratio of ZrCl₄ or HfCl₄ in THF at −78 °C led to colorless crystalline complexes [PhNC-
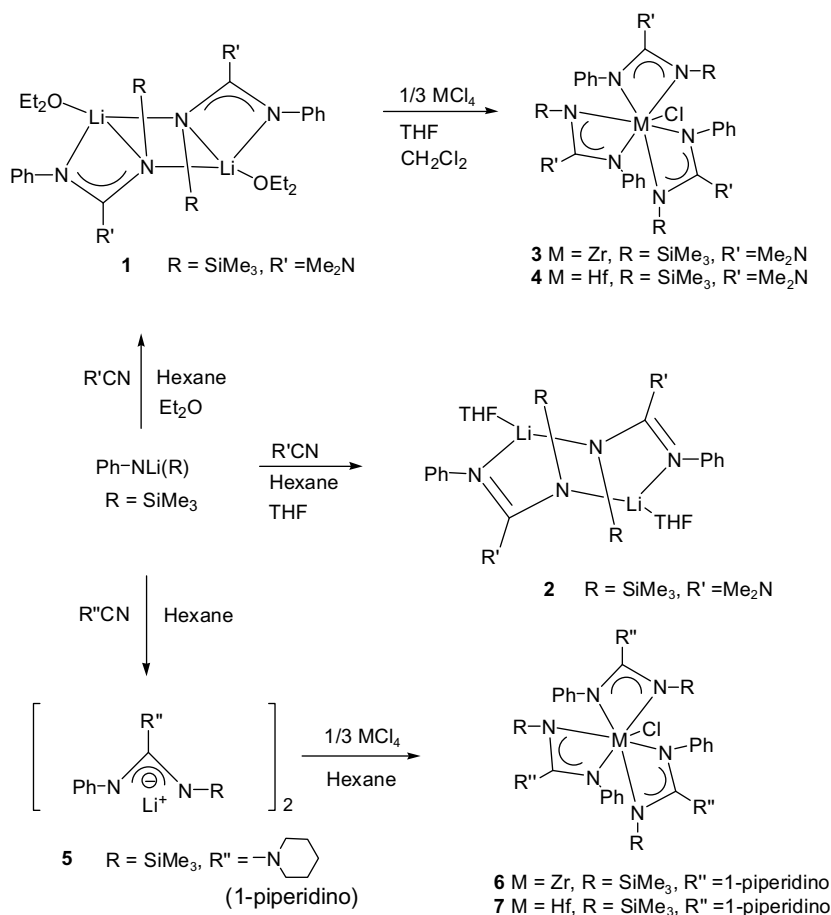
Scheme 1. Synthetic routes to complexes 1–7.

(NMe₂)NSiMe₃]₃ZrCl (**3**) and [PhNC(NMe₂)NSiMe₃]₃ HfCl (**4**), respectively. These complexes could be easily recrystallized to get single crystals suitable for X-ray analysis in dichloromethane. Similarly, the complexes [PhNC(N(CH₂)₅)NSiMe₃]₃ZrCl (**6**) and [PhNC(N(CH₂)₅)-NSiMe₃]₃HfCl (**7**) were obtained by treatment of **5** with one third portion of ZrCl₄ or HfCl₄ in hexane at −78 °C and the single crystals of **7** were obtained from recrystallization in hexane.

2.2. Molecular structures of complexes 1–4 and 7

The molecular structure of crystalline **1** is illustrated in Fig. 1 and the selected bond lengths and angles are listed in Table 1. The molecular structure of **1** is a dimmer built around planar LiNLiN ring and the angles at the nitrogen atom are narrower [73.5(3)°] than those at the Li atom [106.5(3)°]. One lithium atom is coordinated with three N and one O atom (Et₂O). The core of the centrosymmetric molecule **1** has a fused tricyclic ladder motif comprising a central planar N2Li1N2′Li1′ ring flanked by planar N1C1N2Li1 and N1′C1′N2′Li1′ rings. The dihedral angle between them is 63.6°. The electronic delocalization throughout the guanidinate moiety is observed from

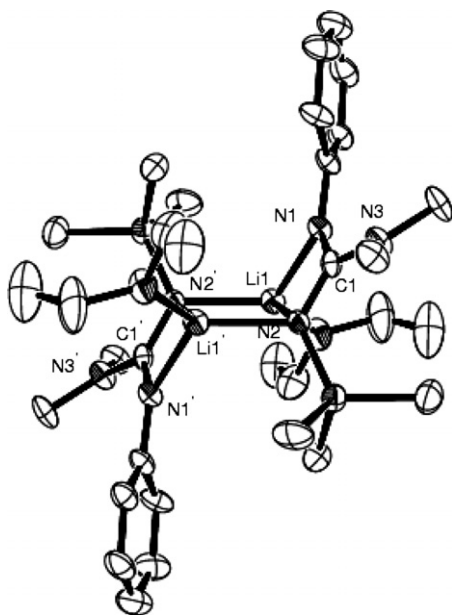the C–N distances [N(1)–C(1) = 1.323(5) Å, N(2)–C(1) = 1.340(5) Å].

The X-ray data for complex **2** is enough to confirm the outline of the molecule but does not meet the standards of the Journal.

An X-ray study of complex **3** (Fig. 2, Table 2) reveals a "propeller"-like structure, in which three ligands as leaf blades with the metal–chloride bond as leafstalk. Owing to the propeller-like structure, three trimethylsilyl groups are located close to the chlorine atom and the three phenyl groups are arranged on the *trans*-position to the chlorine. In complex **3**, the Zr–Cl bond distance [2.515(15) Å] is longer than the corresponding values found for the earlier examples having such structure as L_3ZrCl including symmetric zirconium benzamidinate [(Siam)₃ZrCl] [Siam = N,N′bis(trimethylsilyl)benzamidinat]] [Zr–Cl 2.464(2) Å] [23] and non-symmetric chiral zirconium benzamidinate complex [{C₆H₅C(N-TMS)(N-myrtanyl)}₃ZrCl] [Zr–Cl 2.475(3) Å] [24]. The Zr–N bond lengths of 2.216(4)–2.292(4) Å are consistent with the values previously reported [24,25]. For the CN₃ framework, the three C–N bond distances in the guanidinate ligand are N1–C7
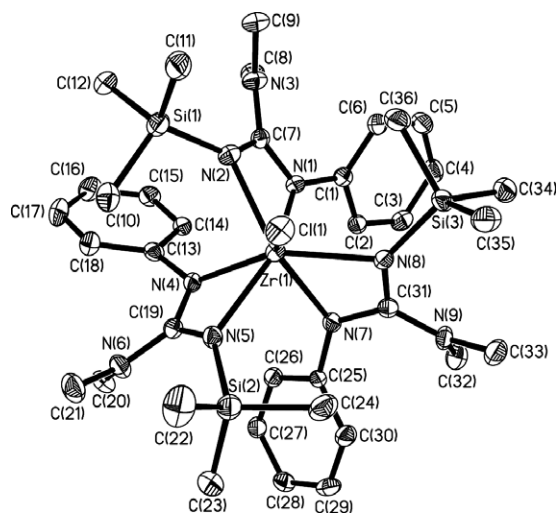

Fig. 2. Molecular structure of compound **3**.

Table 2
Selected bond lengths (Å) and angles (°) of compound **3**

Bond lengths (Å)		Bond angles (°)	
Zr(1)–Cl(1)	2.5151(15)	N(1)–Zr(1)–N(2)	59.24(15)
Zr(1)–N(1)	2.291(4)	N(4)–Zr(1)–N(5)	59.36(14)
Zr(1)–N(2)	2.219(4)	N(7)–Zr(1)–N(8)	59.06(14)
Zr(1)–N(4)	2.285(4)	N(1)–C(7)–N(2)	112.8(5)
Zr(1)– N(5)	2.216(4)	N(4)–C(19)–N(5)	113.3(5)
Zr(1)–N(7)	2.292(4)	N(7)–C(31)–N(8)	112.9(5)
Zr(1)–N(8)	2.217(4)	N(1)–Zr(1)–Cl(1)	128.55(11)
N(1)–C(7)	1.343(6)	N(2)–Zr(1)–Cl(1)	83.17(11)
N(2)–C(7)	1.334(6)	N(4)–Zr(1)–Cl(1)	129.54(11)
N(3)–C(7)	1.378(6)	N(5)–Zr(1)–Cl(1)	83.65(11)
N(6)–C(19)	1.381(6)	N(7)–Zr(1)–Cl(1)	128.65(10)
N(9)–C(31)	1.371(6)	N(8)–Zr(1)–Cl(1)	83.37(11)

Fig. 1. Molecular structure of compound **1**.

Table 1
Selected bond lengths (Å) and angles (°) of compound **1**

Bond lengths (Å)		Bond angles (°)	
C(1)–N(1)	1.323(2)	N(1)–C(1)–N(2)	118.20(14)
C(1)–N(2)	1.341(2)	N(1)–C(1)–N(3)	120.95(12)
C(1)–N(3)	1.391(2)	N(1)–Li(1)–N(2)	65.79(9)
N(1)–Li(1)	1.997(3)	Li(1)–N(2)–Li(1′)	73.56(14)
N(2)– Li(1)	2.201(3)		
N(2′)–Li(1)	2.057(3)		
Li(1)–O(1)	1.977(3)		

1.343(6) Å, N2–C7 1.334(6) Å and N3–C7 1.378(6) Å, respectively. All of these bond distances are roughly in the range for $C(sp^2)$–$N(sp^2)$ bonds (*ca.* 1.36 Å) [26]. This is an indication of lone pair donation from the nitrogen atom (dimethylamido group) to the central carbon and concomitant electron delocalization involving all three nitrogen atoms of the chelating ligand. Complex **4** exhibited geometric and structural feature similar to those of **3**. The molecular structure of crystalline **4** is shown in Fig. 3 and selected bond distances and angles are listed in Table 3. In complex **4**, the bond length of Hf–Cl [2.497(2) Å] is normal as in symmetric guanidinato Hf complex [Hf–Cl = 2.41–2.52 Å] [25]. The bond lengths of Hf–N are in the range of 2.18–2.27 Å; bond lengths of C–N in the guanidinate moiety are in the range of 1.32–1.34 Å. The bond angles of N–C–N are 110.5 (8)°, 112.4 (7)° and 113.1 (7)°, respectively. The dihedral angle between N(1)–Hf(1)–N(3) and N(4)–Hf(1)–N(6) , N(1)–Hf(1)–N(3) and N(7)–Hf(1)–N(9), and N(4)–Hf(1)–N(6) and N(7)–Hf(1)–N(9) are 91.2°, 91.3° and 88.6°, respectively.

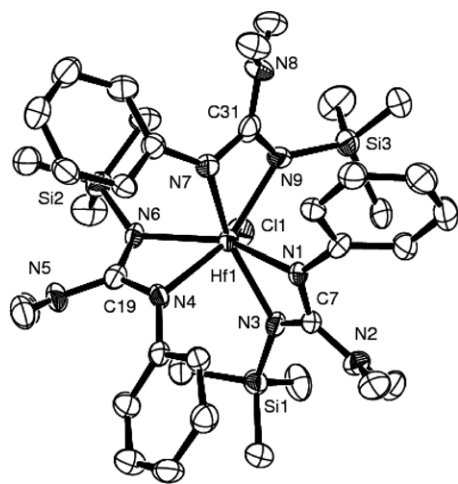The dihedral angle formed by the planar NMe$_2$ function and the MNCN plane offers a means of evaluating the possibility of π overlap between these two moieties. In the case of **3** and **4**, the torsional angles between these two planes are 40.3° (**3**) and 39.8° (**4**), respectively. They are much smaller than that in [{^{i}PrNC[N(SiMe$_3$)$_2$]-N^{i}Pr}$_2$ZrCl$_2$] [88.2°], [{CyNC[N(SiMe$_3$)$_2$]NCy}$_2$ZrCl$_2$] [86.3°] or [{CyNC[N(SiMe$_3$)$_2$]NCy}$_2$HfCl$_2$] [85.8°] [25], suggest that the steric interaction between the phenyl or trimethylsilyl and the dimethylamido group is somewhat limited and is not big enough to eliminate the π conjugation. In fact, the sum of 359.8° (**3**) and 359.9° (**4**) for the three bond angles around N atom in dimethylamido group are consistent with the sp^2 hybridization necessary for conjugation.

Crystals of **6**, obtained from hexane, were of poor quality but the data were adequate to establish its structure as shown in Scheme 1. In complex **7** (Fig. 4, Table 4), there are two independent molecules in the unit cell and the bond distances and angles have no significant differences. Therefore, bond lengths and angles in one molecule were listed. The molecule shows similar geometric and structural features to those of **3** and **4**, i.e. a capped octahedral structure
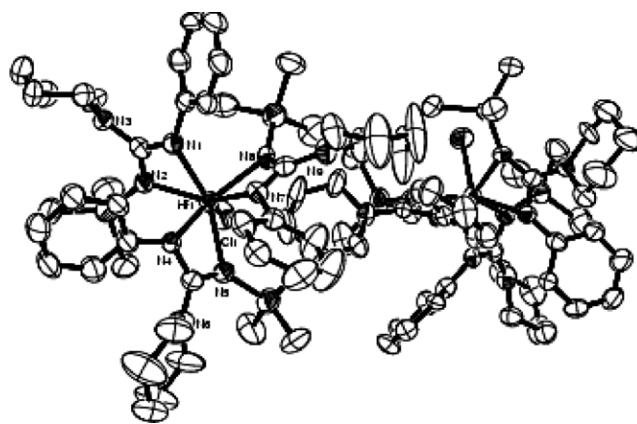

Fig. 3. Molecular structure of compound **4**.

Fig. 4. Molecular structure of compound **7**.

Table 3
Selected bond lengths (Å) and angles (°) of compound **4**

Bond lengths (Å)		Bond angles (°)	
Hf(1)–Cl(1)	2.497(2)	N(1)–Hf(1)–N(3)	59.7(2)
Hf(1)–N(1)	2.265(6)	N(4)–Hf(1)–N(6)	59.6(2)
Hf(1)–N(3)	2.194(7)	N(7)–Hf(1)–N(9)	59.7(2)
Hf(1)–N(4)	2.276(6)	N(1)–C(7)–N(3)	112.4(7)
Hf(1)–N(6)	2.199(6)	N(4)–C(19)–N(6)	113.1(7)
Hf(1)–N(7)	2.262(7)	N(7)–C(31)–N(9)	110.5(8)
Hf(1)–N(9)	2.186(7)	N(1)–Hf(1)–Cl(1)	128.56(18)
N(1)–C(7)	1.346(11)	N(3)–Hf(1)–Cl(1)	82.79(19)
N(3)–C(7)	1.326(11)	N(4)–Hf(1)–Cl(1)	128.59(18)
N(2)–C(7)	1.365(11)	N(6)–Hf(1)–Cl(1)	82.94(18)
N(5)–C(19)	1.381(11)	N(7)–Hf(1)–Cl(1)	129.36(18)
N(8)–C(31)	1.349(12)	N(9)–Hf(1)–Cl(1)	83.32(19)

Table 4
Selected bond lengths (Å) and angles (°) of compound **7**

Bond lengths (Å)		Bond angles (°)	
Hf(1)–Cl(1)	2.475(3)	N(1)–Hf(1)–N(2)	59.3(3)
Hf(1)–N(1)	2.240(8)	N(4)–Hf(1)–N(5)	59.3(3)
Hf(1)–N(2)	2.214(8)	N(7)–Hf(1)–N(8)	59.5(3)
Hf(1)–N(4)	2.244(7)	N(1)–C(1)–N(2)	113.3(10)
Hf(1)–N(5)	2.229(8)	N(4)–C(16)–N(5)	111.5(10)
Hf(1)–N(7)	2.248(8)	N(7)–C(31)–N(8)	110.6(10)
Hf(1)–N(8)	2.224(8)	N(1)–Hf(1)–Cl(1)	127.1(2)
N(3)–C(1)	1.401(12)	N(2)–Hf(1)–Cl(1)	82.7(2)
N(6)–C(16)	1.387(13)	N(4)–Hf(1)–Cl(1)	129.4(2)
N(9)–C(31)	1.369(13)	N(5)–Hf(1)–Cl(1)	84.4(2)
N(1)–C(1)	1.330(12)	N(7)–Hf(1)–Cl(1)	130.7(2)
N(2)–C(1)	1.309(11)	N(8)–Hf(1)–Cl(1)	83.7(2)
N(4)–C(16)	1.346(11)		
N(5)–C(16)	1.328(12)		
N(7)–C(31)	1.343(12)		
N(8)–C(31)	1.356(13)		

with the coordination number 7 at the hafnium. The bond distance of C(central)–N(1-piperidino) [1.401(12) Å] in **7** is longer than C(central)–N(dimethylamido) [1.3786 Å] in **3** and [1.365(11) Å] in **4**, but similar to that in Hf{[C$_6$H$_{11}$NC-(N(Si(CH$_3$)$_3$)$_2$)NC$_6$H$_{11}$]Cl$_4$}{Li(THF)$_3$} [1.41(2) Å] [25]. The 1-piperidino ring in **7** adopts a chair conformation. Although the dihedral angle [48.9°] between the chelating core N–C–N and its adjacent C–N–C plane of 1-piperidino group is larger than that in **3** and **4**, which suggests more bulky 1-piperidino group than dimethylamido group, the sum of 355.4° for the three bond angles around 1-piperidino N atom indicates the strong π-bonding interaction between the two moieties as well.

2.3. The ethylene polymerization reaction activated by 3, 4, 6 and 7

The influences of various catalytic systems formed from **3**, **4**, **6** and **7** in the presence of cocatalysts such as methylaluminoxane (MAO) or Et$_2$AlCl on the ethylene activation were evaluated. To demonstrate what factors, and how they may affect the ethylene polymerization, the activity of catalyst precursor **4** was particularly investigated at varied Al/Hf molar ratio and temperature. The detailed results are summarized in Table 5.

At atmospheric pressure of ethylene, complex **3** has not been found to be active for the polymerization of ethylene, no matter activated with MAO or Et$_2$AlCl, neither with Et$_2$AlCl under 10 atm of ethylene. Based on this observation, 10 atm pressure of ethylene was employed in the experiments, in which other reaction parameters were varied. For complexes **3** and **4**, larger amounts of MAO were found to decrease the activity, at a ratio of Al/M 1000 reaching higher activities 1.05×10^4 and 2.92×10^4 g mol^{-1} h^{-1}, respectively. Therefore, ethylene polymerization reactions were carried out under 10 atm of ethylene at Al/M ratio of 1000 at room temperature for complexes **3**, **4**, **6** and **7**, activated with MAO. As shown in Table 5, complex **3**, **4**, **6** and **7** were active for the polymerization of ethylene with the order of **4** > **6** > **3** > **7**. So complex **4** was selected for a series of polymerizations at varied reaction temperature from 20 to 80 °C while other reaction parameters were not changed. Apparently, the activity of the catalyst decreased in this whole process with increased reaction temperature. With the temperature from 20 to 80 °C, the activity of **4** decreased from 2.92×10^4 to 1.15×10^4 g PE mol^{-1} h^{-1}. Overall, the catalytic system displays good activity over a wide range of reaction temperature. Molecular weight, on the other hand, increased as temperature was raised. This suggests that single molecule might show higher catalytic activity at higher temperature, although deactivation or decomposition proceeds faster at higher temperature.

In our case, the change of ligands and central metals did not affect the catalytic activity of the compounds significantly. Complex **6** with 1-piperidino group on guanidine showed a catalytic activity of 1.52×10^4 g mol^{-1} h^{-1} while **3** with *N,N*-dimethyl group on guanidine showed a relatively lower value of 1.05×10^4 g mol^{-1} h^{-1}; as for complexes **3** and **4**, the hafnium guanidine **4** showed a relatively higher catalytic activity of 2.92×10^4 g mol^{-1} h^{-1} than the corresponding zirconium guanidine **3** (1.05×10^4 g mol^{-1} h^{-1}). The angle between the propeller flaps in complex **4** [91.2°] is larger by 2.4° than that in complex **3** [88.8°], resulting in a more exposed chloride ligand. This opened coordination is likely partially responsible for the different catalytic activity.

Comparing with the analogue zirconium benzamidinate complex [Zr(κ^2-L)$_3$Cl] (**L** = [N(SiMe$_3$)C(C$_6$H$_4$Me-4)NPh]$^-$) [27], complex **3** exhibited lower activity for ethylene polymerization. The difference between the activities of the two complexes could be due to the electronic factor of the ligands. In complex **3**, dimethylamido group could be a stronger donor (more basic) than the analogue amidinate complex and, for the given zirconium metal, replacement of

Table 5
Data for ethylene polymerization catalyzed by complexes **3**, **4**, **6** and **7**/cocat system

Entry	Cat	Cocat	P (atm)	T (°C)	Al/Zr(Hf)	Yield (mg)	Activity[a]	M_η (10^4)[b]
1	**3**	MAO	1	20	1000	–	No	–
2	**3**	Et$_2$AlCl	1	20	500	–	No	–
3	**3**	Et$_2$AlCl	10	20	500	–	No	–
4	**3**	MAO	10	20	1000	26.2	1.05×10^4	1.8
5	**3**	MAO	10	20	2000	–	Trace	–
6	**4**	MAO	10	20	500	–	Trace	–
7	**4**	MAO	10	20	1000	73.0	2.92×10^4	1.1
8	**4**	MAO	10	20	1500	26.9	1.08×10^4	1.3
9	**4**	MAO	10	20	2000	26.7	1.07×10^4	4.9
10	**4**	MAO	10	40	1000	69.4	2.78×10^4	28
11	**4**	MAO	10	60	1000	41.6	1.67×10^4	35
12	**4**	MAO	10	80	1000	28.7	1.15×10^4	34
13	**6**	MAO	10	20	1000	38.0	1.52×10^4	–
14	**7**	MAO	10	20	1000	23.7	9.48×10^3	0.35

Conditions: 5 μmol catalyst, 30 ml toluene for 1 atm ethylene pressure, 100 ml toluene for 10 atm ethylene pressure, 0.5 h.
[a] g mol^{-1} h^{-1}.
[b] Measured in decahydronaphthalene at 135 °C using an Ubbelohde viscometer according to $[\eta] = 62 \times 10^{-3} M_\eta^{0.7}$.

an amidinate by a guanidinate increased the electron density on the metal and reduced its catalytic activity for ethylene polymerization.

3. Experimental

3.1. General remarks

All manipulations were performed under argon using standard Schlenk and vacuum line techniques [28,29]. Solvents were dried and distilled over Na or Na/K alloy under argon prior to use. Methylaluminoxane (MAO, 1.46 M solution in toluene) was purchased from Akzo Nobel Corp. Diethylaluminum chloride (Et_2AlCl, 1.7 M in toluene) and other reagents were purchased from Acros or Aldrich. $PhNHSiMe_3$ was prepared according to the literature [30]. The NMR spectra were recorded on a Bruker DKX-300 instrument, and solvent resonances were used as the internal references for ^1H spectra and ^{13}C spectra. Elemental analyses were carried out using a Vario EL-III analyzer (Germany).

3.2. Preparations

3.2.1. $[(Et_2O)LiN(SiMe_3)C(NMe_2)N(Ph)]_2$ (1) and $[(THF)LiN(SiMe_3)C(NMe_2)N(Ph)]_2$ (2)

The reaction of $PhNHSiMe_3$ with *n*-butyllithium at the ratio of 1:1 in hexane at 0 °C affords $PhN(Li)SiMe_3$ in 80% yield. $(CH_3)_2NCN$ (0.73 ml, 9.08 mmol) was added to a solution of $PhN(Li)SiMe_3$ (1.5 g, 9.08 mmol) in hexane (20 ml) at −78 °C. The resulting mixture was warmed to *ca.* 25 °C and stirred for overnight. The volatiles were removed *in vacuo* and the residue was recrystallised from Et_2O yielding colorless crystals of compound 1 (0.96 g, 44%). ^1H NMR (C_6D_6): δ 0.23 (s, 9H, $SiMe_3$), 2.70 (s, 6H, NMe), 6.91–7.07 (m, 2H, Ph), 7.27–7.50 (m, 3H, Ph). ^{13}C NMR (C_6D_6): δ 5.5 (s, $SiMe_3$), 40.3 (s, NMe), 127–130 (m, Ph), 155.8 (s, $C(C_5H_5)$), 183.6 (s, N$C(NMe_2)$N). Crystallization from THF yielded colorless crystals of compound 2 (80%). ^1H NMR (C_6D_6): δ 0.42 (s, 9H, $SiMe_3$), 2.71–2.80 (d, 6H, NMe), 1.43, 1.45, 1.47 (thf), 3.61, 3.64, 3.66 (thf), 6.85–7.32 (m, 5H, Ph). ^{13}C NMR (C_6D_6): δ 5.74 (s, $SiMe_3$), 41.1–41.9 (s, NMe), 28.1, 70.4 (thf), 120.7–156.0 (m, Ph), 166.8 (s, $C(C_5H_5)$), 170.4 (s, N$C(NMe_2)$N).

3.2.2. $[PhNC(NMe_2)NSiMe_3]_3ZrCl \cdot 2CH_2Cl_2$ (3)

$(CH_3)_2NCN$ (0.32 ml, 4.00 mmol) was added to a solution of $PhN(Li)SiMe_3$ (0.68 g, 4.00 mmol) in THF (30 cm^3) at −78 °C. The resulting mixture was warmed to *ca.* 25 °C and stirred for overnight. $ZrCl_4$ (0.10 g, 1.33 mmol) was added at −78 °C. The resulting mixture was warmed to *ca.* 25 °C and stirred for 60 h. The volatiles were removed *in vacuo*, and the residue was extracted with dichloromethane and filtered. The filtrate was concentrated to give colorless crystals of 3 (0.49 g, 44%). Anal. Cacl. for $C_{38}H_{64}Cl_5N_9Si_3Zr$: C, 45.74; H, 6.46; N, 12.60. Found: C, 46.00; H, 6.52; N, 12.84%. ^1H NMR (CDCl$_3$): δ 0.04 (s,

9H, $SiMe_3$), 2.40 (s, 6H, NMe), 6.8–7.1 (m, 5H, Ph). ^{13}C NMR (CDCl$_3$): δ 2.37 (s, $SiMe_3$), 39.6 (s, NMe), 121 (s, Ph), 123 (s, Ph), 127 (s, Ph), 147 (s, $C(C_5H_5)$), 167 (s, N$C(NMe_2)$N).

3.2.3. $[PhNC(NMe_2)NSiMe_3]_3HfCl \cdot 2CH_2Cl_2$ (4)

$(CH_3)_2NCN$ (0.30 ml, 3.68 mmol) was added to a solution of $PhN(Li)SiMe_3$ (0.63 g, 3.68 mmol) in THF (30 cm^3) at −78 °C. The resulting mixture was warmed to *ca.* 25 °C and stirred for overnight. $HfCl_4$ (0.39 g, 1.23 mmol) was added at −78 °C. The resulting mixture was warmed to *ca.* 25 °C and stirred for 60 h. The volatiles were removed in *vacuo*, and the residue was extracted with dichloromethane and filtered. The filtrate was concentrated to give colorless crystals of 4 (0.48 g, 36%). Anal. Cacl. for $C_{38}H_{64}Cl_5N_9Si_3Hf$: C, 41.99; H, 5.93; N, 11.60. Found: C, 41.79; H, 6.10; N, 11.42%. ^1H NMR (CDCl$_3$): δ 0.05 (s, 9H, $SiMe_3$), δ 2.40 (s, 6H, NMe), δ 6.8–7.2 (m, 5H, Ph). ^{13}C NMR (CDCl$_3$): δ 2.51 (s, $SiMe_3$), δ 39.7 (s, NMe), δ 121 (s, Ph), δ 123 (s, Ph), δ 127 (s, Ph), δ 147 (s, $C(C_5H_5)$), δ 167 (s, N$C(NMe_2)$N).

3.2.4. $[PhNC(\overline{N(CH_2)_4CH_2})NSiMe_3]_3ZrCl$ (6)

1-Piperidinecarbonitrile (0.39 ml, 3.38 mmol) was added to a solution of $PhN(Li)SiMe_3$ (0.58 g, 3.38 mmol) in hexane (30 cm^3) at −78 °C. The resulting mixture was warmed to *ca.* 25 °C and stirred for overnight. $ZrCl_4$ (0.262 g, 1.13 mmol) was added at −78 °C. The resulting mixture was warmed to *ca.* 25 °C and stirred for 12 h, then filtered. The filtrate was concentrated to *ca.* to 15 cm^3 to give colorless crystals of 6 (0.48 g, 45%). Anal. Cacl. for $C_{45}H_{72}ClZrN_9Si_3$: C, 56.89; H, 7.64; N, 13.27. Found: C, 56.67; H, 7.65; N, 13.03%. ^1H NMR (CDCl$_3$): δ 0.196 (s, 9H, $SiMe_3$), δ 1.16 (s, 2H, CH_2), δ 1.31 (s, 4H, CH_2), δ 2.57–2.61 (d, 2H, CH_2), δ 2.74–2.80 (t, 2H, CH_2), δ 6.83–6.88 (t, 1H, Ph), δ 7.01–7.04 (d, 2H, Ph), δ 7.08–7.13 (t, 2H, Ph). ^{13}C NMR (CDCl$_3$): δ 3.13 (s, $SiMe_3$), δ 23.8, 24.1, 48.2(3s, CH_2), δ 121, 124, 127 (3s, Ph), δ 147 (s, $C(C_5H_5)$), δ 167 (s, NC(1-piperidino)N).

3.2.5. $[PhNC(\overline{N(CH_2)_4CH_2})NSiMe_3]_3HfCl$ (7)

1-Piperidinecarbonitrile (0.32 ml, 2.77 mmol) was added to a solution of $PhN(Li)SiMe_3$ (0.47 g, 2.77 mmol) in hexane (30 cm^3) at −78 °C. The resulting mixture was warmed to *ca.* 25 °C and stirred for overnight. $HfCl_4$ (0.30 g, 0.92 mmol) was added at −78 °C. The resulting mixture was warmed to *ca.* 25 °C and stirred for 12 h, then filtered. The filtrate was concentrated to *ca.* to 15 cm^3 to give colorless crystals of 7 (0.32 g, 33%). Anal. Cacl. for $C_{45}H_{72}ClHfN_9Si_3$: C, 52.10; H, 7.00; N, 12.15. Found: C, 52.00; H, 7.03; N, 11.98%. ^1H NMR (CDCl$_3$): δ 0.19 (s, 9H, $SiMe_3$), δ 1.15 (s, 2H, CH_2), δ 1.32 (s, 4H, CH_2), δ 2.58–2.62 (d, 2H, CH_2), δ 2.75–2.81 (t, 2H, CH_2), δ 6.83–6.87 (t, 1H, Ph), δ 7.02–7.05 (d, 2H, Ph), δ 7.09–7.14 (t, 2H, Ph). ^{13}C NMR (CDCl$_3$): δ 3.72 (s, $SiMe_3$), δ 24.2, 24.5, 48.7 (3s, CH_2), δ 121, 125, 127 (3s, Ph), δ 147 (s, $C(C_5H_5)$), δ 167 (s, NC(1-piperidino)N).

Table 6
Crystal and refinement data for **1**, **3**, **4** and **7**

Compound	1	3	4	7
Formula	$C_{32}H_{60}Li_2N_6O_2Si_2$	$C_{38}H_{64}Cl_5N_9Si_3Zr$	$C_{38}H_{64}Cl_5HfN_9Si_3$	$C_{45}H_{72}ClHfN_9Si_3$
M	630.92	999.72	1086.99	1037.33
Crystal system	Monoclinic	Triclinic	Triclinic	Monoclinic
Space group	$p2(1)/c$	$P\bar{1}$ (No. 2)	$P\bar{1}$ (No. 2)	$P2(1)/c$
a (Å)	10.052(8)	11.953(3)	11.894(2)	22.209(13)
b (Å)	20.114(19)	12.995(3)	12.961(3)	23.699(14)
c (Å)	10.926(12)	17.508(4)	17.507(3)	19.699(12)
α (°)	90.00	71.048(3)	70.939(2)	90.00
β (°)	114.967(11)	76.964(3)	77.232(3)	92.057(10)
γ (°)	90.00	81.753(3)	81.657(3)	90.00
U (Å^3)	2003(3)	2498.6(9)	2480.0(9)	10362(11)
Z	2	2	2	8
Absorption coefficient (mm^{-1})	0.121	0.596	2.482	2.173
Unique reflections [R_{int}]	3519 [0.098]	8632 [0.061]	8559 [0.036]	18178 [0.130]
Reflections with $I > 2\sigma(I)$	1544	4500	7594	1081
Final R indices [$I > 2\sigma(I)$] R_1, wR_2	0.074, 0.1228	0.061, 0.1043	0.070, 0.1543	0.062, 0.1218
R indices (all data) R_1, wR_2	0.1720, 0.1527	0.1147, 0.1188	0.080, 0.1594	0.1640, 0.1660

3.2.6. Procedure for ethylene polymerization

Ethylene polymerization at 1 atm of ethylene pressure was carried out as follows: The catalyst precursor was dissolved in toluene in a Schlenk tube and the reaction solution was stirred at 1 atm of ethylene. The reaction was initiated by adding the desired amount of cocatalyst. After 30 min, the solution was quenched with HCl–acidified ethanol (5%), and the precipitated polyethylene was filtered, washed with ethanol, and dried in vacuum at 60 °C to constant weight.

Ethylene polymerization at higher ethylene pressure was carried out in a 500 ml autoclave stainless steel reactor equipped with a mechanical stirrer and a temperature controller. Briefly, toluene, the desired amount of cocatalyst, and a toluene solution of the catalytic precursor (the total volume was 100 ml) were added to the reactor in this order under an ethylene atmosphere. When the desired reaction temperature was reached, ethylene at 10 atm pressure was introduced to start the reaction, and the ethylene pressure was maintained by constant feeding of ethylene. After 30 min, the reaction was stopped. The solution was quenched with HCl–acidified ethanol (5%), and the precipitated polyethylene was filtered, washed with ethanol, and dried in vacuum at 60 °C to constant weight.

3.3. X-ray crystal data and refinement for 1, 3, 4 and 7

Diffraction data for each of **1**, **3**,**4** and **7** were collected on a Bruker SMART APEX diffractometer/CCD area detector using monochromated Mo Kα radiation, $\lambda = 0.71073$ Å. Crystals were coated in oil and then directly mounted on the diffractometer under a stream of cold nitrogen gas. A total of N reflections were collected by using ω scan mode. Corrections were applied for Lorentz and polarization effects as well as absorption using multi-scans (SADABS) [31]. The structure was solved by direct method (SHELXS-97) [32]. Then the remaining non-hydrogen atoms were obtained from the successive difference fourier map. All non-H atoms were refined with anisotropic displacement parameters, while the H atoms were constrained to parent sites, using a riding mode (SHELXTL) [33]. Crystal data and processing parameters for **1**, **3**, **4** and **7** are summarized in Table 6.

Acknowledgements

Appendix A. Supplementary material

CCDC 195471, 203550, 603753, 603754 and 631436 contain the supplementary crystallographic data for **1**, **2**, **3**, **4** and **7**. These data can be obtained free of charge via http://www.ccdc.cam.ac.uk/conts/retrieving.html, or from the Cambridge Crystallographic Data Centre, 12 Union Road, Cambridge CB2 1EZ, UK, fax: (+44) 1223-336-033, or e-mail: deposit@ccdc.cam.ac.uk. Supplementary data associated with this article can be found, in the online version, at doi:10.1016/j.jorganchem.2007.07.051.

References

[1] (a) P.J. Bailey, S. Pace, Coord. Chem. Rev. 214 (2001) 91;
(b) F.T. Edelmann, Coord.Chem. Rev. 137 (1994) 403.
[2] Li-Ying Zhou, Hong-Mei Sun, Jing-Lei Chen, Ying-Ming Yao, Qi Shen, J. Polym. Sci. Part A: Polym. Chem. 43 (2005) 1778.
[3] P. Bazinet, D. Wood, G.P.A. Yap, D.S. Richeson, Inorg. Chem. 42 (2003) 6225.
[4] Yun-Jie Luo, Ying-Ming Yao, Qi Shen, Macromolecules 35 (2002) 8670.

[5] M.P. Coles, Dalton Trans. (2006) 985.

[6] J. Barker, M. Kilner, Coord. Chem. Rev. 133 (1994) 219.

[7] D.H. Korine, M.S. Eisen, J. Organomet. Chem. 503 (1995) 307.

[8] A.P. Duncan, S.M. Mullins, J. Arnold, R.G. Bergman, Organometallics 20 (2001) 1808.

[9] (a) R.J. Keaton, L.A. Koterwas, J.C. Fettinger, L.R. Sita, J. Am. Chem. Soc. 124 (2002) 5932;
(b) R.J. Keaton, L.R. Sita, Organometallics 21 (2002) 4315;
(c) R.J. Keaton, K.C. Jayaratne, D.A. Henningsen, L.A. Koterwas, L.R. Sita, J. Am. Chem. Soc. 123 (2001) 6197.

[10] Tiow-Gan Ong, G.P.A. Yap, D.S. Richeson, Organometallics 21 (2002) 2839.

[11] A. Devi, R. Bhakta, A. Milanov, M. Hellwig, D. Barreca, E. Tondello, R. Thomas, P. Ehrhart, M. Winter, R. Fischer, Dalton Trans. (2007) 1671.

[12] Tiow-Gan Ong, G.P.A. Yap, D.S. Richeson, Organometallics 22 (2003) 387.

[13] Mei-Su Zhou, Shu-Ping Huang, Lin-Hong Weng, Wen-Hua Sun, Dian-Sheng Liu, J. Organomet. Chem. 665 (2003) 237.

[14] Sheng-Di Bai, Jian-Ping Guo, Dian-Sheng Liu, Dalton Trans. (2006) 2244.

[15] Sheng-Di Bai, Jian-Ping Guo, Dian-Sheng Liu, W.Y. Wong, Eur. J. Inorg. Chem. (2006) 4903.

[16] Jian-Feng Li, Shu-Ping Huang, Lin-Hong Weng, Dian-Sheng Liu, J. Organomet. Chem. 691 (2006) 3003.

[17] S.E. Schaus, J. Branalt, E.N. Jacobsen, J. Org. Chem. 63 (1998) 403.

[18] B.M. Trost, M.J. Krische, R. Radinov, G. Zanoni, J. Am. Chem. Soc. 118 (1996) 6297.

[19] Jie Zhang, Rui-Fang Cai, Lin-Hong Weng, Xi-Geng Zhou, J. Organomet. Chem. 672 (2003) 94.

[20] B.W. Corey, L.R. Laurel, A.A. Khalil, M.W. Lisa, Inorg. Chem. 45 (2006) 263.

[21] R. Daniel, B. Arne, W. Manuela, A.F. Roland, Inorg. Chem. 45 (2006) 269.

[22] M.P. Coles, P.B. Hitchcock, Eur. J. Inorg. Chem. (2004) 2662.

[23] D. Walther, R. Fischer, H. Görls, J. Koch, B. Schweder, J. Organomet. Chem. 508 (1996) 13.

[24] C. Averbuj, E. Tish, M.S. Eisen, J. Am. Chem. Soc. 120 (1998) 8640.

[25] D. Wood, G.P.A. Yap, D.S. Richeson, Inorg. Chem. 38 (1999) 5788.

[26] F.H. Allen, O. Kennard, D.G. Watson, L. Brammer, A.G. Orpen, R. Taylor, J. Chem. Soc., Perkin Trans. 2 (1987) S1.

[27] P.B. Hitchcock, M.F. Lappert, P.G. Merle, Dalton Trans. (2007) 585.

[28] D.F. Shriver, M.A. Drezdon, The Manipulation of Air Sensitive Compounds, second ed., Wiley, New York, 1986.

[29] S. Herzog, J. Dehnert, K. LuhderTechnique of Inorganic Chemistry, vol. VII, Interscience, New York, 1969.

[30] H.H. Anderson, J. Am. Chem. Soc. 73 (1951) 5802.

[31] G.M. Sheldrick, Correction Software, University of Göttinggen, Germany, 1996.

[32] G.M. Sheldrick, Program for the Solution of Crystal Structures, University of Göttinggen, Germany, 1997.

[33] Program for Crystal Structure Refinement, Bruker Analytical X-ray Instruments Inc., Madison, WI, USA, 1998.